

## Fabrication of Cu<sub>2</sub>O/ $\gamma$ -FeOOH Heterojunction Solar Cells by Electrodeposition

Junie Jhon M. Vequizo<sup>1,2</sup> and Masaya Ichimura<sup>1,\*</sup>

<sup>1</sup>Department of Engineering Physics, Electronics and Mechanics, Nagoya Institute of Technology, Gokiso, Showa, Nagoya 466-8555, Japan

<sup>2</sup>Department of Physics, College of Science and Mathematics, Western Mindanao State University, Zamboanga City 7000, Philippines

Cu<sub>2</sub>O/ $\gamma$ -FeOOH heterojunction solar cells were fabricated by galvanostatic-potentiostatic electrodeposition methods. The  $\gamma$ -FeOOH films showed n-type conductivity with band gap of 2.2 eV. The electrodeposited Cu<sub>2</sub>O/ $\gamma$ -FeOOH heterojunction exhibited photovoltaic characteristics with short circuit current density of 0.95 mA/cm<sup>2</sup> and open circuit voltage of 0.11 V. From core level spectroscopy, the Cu<sub>2</sub>O/FeOOH heterostructure displayed a type II junction with valence band offset of 0.8 eV. The conduction band minimum of Cu<sub>2</sub>O was predicted to be higher than that of  $\gamma$ -FeOOH by 0.7 eV. With this finding, the  $\gamma$ -FeOOH material may be regarded as a suitable candidate for hetero-partner of other p-type absorbers.

\* Corresponding author: [ichimura.masaya@nitech.ac.jp](mailto:ichimura.masaya@nitech.ac.jp)

The interesting characteristics of oxide semiconductors such as copper oxide ( $\text{Cu}_2\text{O}$ ) and iron oxide ( $\text{Fe}_2\text{O}_3$ ) have stimulated extensive research on the potential materials for wide range of device applications (e.g. photocatalyst, solar cells, etc.) due to the abundance of their components, environmentally-friendly character, and suitable electronic and optical properties. In addition, many kinds of oxide thin films can be prepared with ease by employing simple electrodeposition technique.  $\text{Cu}_2\text{O}$  (with direct band gap,  $E_g = 2.0 - 2.1$  eV) has been regarded as an attractive p-type absorber material in heterojunction solar cells.<sup>1-5)</sup> Numerous efforts have been carried out to fabricate heterostructure solar cells based on  $\text{Cu}_2\text{O}$  with several window layers such as  $\text{ZnO}$ <sup>6-14)</sup>,  $\text{Ga}_2\text{O}_3$ <sup>15)</sup> and  $\text{SnO}_2$ <sup>16)</sup>. Meanwhile,  $\text{Fe}_2\text{O}_3$  is an n-type semiconductor and has been popular as a photocatalytic material, but has never been applied for heterostructure solar cells. Iron oxide hydroxide ( $\text{FeOOH}$ ) has been utilized as a starting precursor to produce  $\gamma\text{-Fe}_2\text{O}_3$  and  $\alpha\text{-Fe}_2\text{O}_3$  via thermal annealing at different temperatures.<sup>17)</sup> Additionally,  $\gamma\text{-FeOOH}$  material has also shown promising contributions as photocatalyst combined with  $\text{TiO}_2$ <sup>18)</sup> and adsorbent materials for heavy ions removals<sup>19)</sup>. Recently, we reported the n-type semiconductor properties of  $\gamma\text{-FeOOH}$  thin films electrodeposited from oxygen-bubbled aqueous solutions at room temperature.<sup>20)</sup> It was found that the electrodeposited  $\gamma\text{-FeOOH}$  exhibits n-type conductivity with a band gap  $> 2$  eV.

In this work, the  $\text{Cu}_2\text{O}/\gamma\text{-FeOOH}$  heterostructure is fabricated by galvanostatic-potentiostatic electrodeposition methods, and the photovoltaic performance as well as the band alignment at the interface are evaluated and investigated for the first time. To our knowledge, no studies have been performed to utilize Fe-based compounds as the n-type layer in a p-n heterojunction. Thus, this paper is the first report on the fabrication of p-n junction using iron oxide/oxyhydroxide compound as one of the components. Our results demonstrate that the usage of  $\gamma\text{-FeOOH}$  as a buffer layer in heterojunction solar cells is possible. Thus, since iron is non-toxic and one of the most abundant elements on earth,  $\gamma\text{-FeOOH}$  can also be a good hetero-partner for other p-type absorbers as an alternative replacement to the popular but highly toxic CdS.

All the electrodeposition experiments were carried out in a three-electrode electrochemical cell with indium tin oxide (ITO)-coated glass substrate, platinum (Pt) sheet, and saturated calomel electrode (SCE) as working, counter and reference electrodes, respectively. Initially,  $\gamma\text{-FeOOH}$  thin films were potentiostatically electrodeposited on the pre-cleaned ITO substrate from acidic aqueous solutions containing 0.05 M  $\text{FeSO}_4$  and 0.1 M  $\text{Na}_2\text{SO}_4$ . The applied potential was -0.9 (V vs SCE).

Modifications in the deposition condition as reported in our previous work on electrodeposition of  $\gamma$ -FeOOH<sup>20)</sup> were made in the current experimental conditions with the following considerations to improve the properties of the film: (a) Na<sub>2</sub>SO<sub>4</sub> was used instead of KCl to ensure homogeneity in the anions and avoid the possible inclusion of Cl<sup>-</sup> during the formation of  $\gamma$ -FeOOH film and (b) solution was stirred during the entire deposition process. As a result, an enhanced current density and thicker films were easily obtainable. A 50-nm thick  $\gamma$ -FeOOH film was used in the fabrication of the p-n junction. Cu<sub>2</sub>O layer was galvanostatically deposited onto the as-prepared  $\gamma$ -FeOOH film from the solution containing 0.2 M CuSO<sub>4</sub> - 1.6 M C<sub>3</sub>H<sub>6</sub>O<sub>3</sub> (pH was adjusted to 12.5 using KOH) with constant cathodic current density (-1.0 mA/cm<sup>2</sup>) at solution temperature of 40°C. The deposition duration for the Cu<sub>2</sub>O layer was maintained at 10 min. This Cu<sub>2</sub>O deposition condition is similar to our previous report on Cu<sub>2</sub>O/ZnO heterojunction.<sup>14)</sup> Since there are numerous studies that performed and reported extensive characterizations on Cu<sub>2</sub>O thin films, only the  $\gamma$ -FeOOH material undergone additional characterizations such as compositional, optical transmission, and photoelectrochemical (PEC) analyses as part of our continuous investigation to improve its properties. Compositional analysis was performed using a JEOL JAMP-9500F field-emission Auger electron spectroscopy (AES). Argon ion etching was done using an acceleration voltage of 2 kV with ion current of 2.6  $\mu$ A to sputter the film's surface. The chemical state of the elements was determined by performing the X-ray photoelectron spectroscopic (XPS) analysis using the XPS PHI-5000 (ULVAC-PHI) with Al K $\alpha$  as the X-ray source. The optical characterization was carried out using a JASCO U-570 ultraviolet/visible/near infrared (UV/vis/NIR) spectrometer from 300-1000 nm in referenced to the substrate. To determine the conductivity type and photoresponse, photoelectrochemical (PEC) measurement was performed in a three-electrode electrochemical cell using 0.1 M Na<sub>2</sub>SO<sub>4</sub> as the electrolyte and the voltage was scanned linearly towards the forward bias region. The sample was illuminated from the substrate side to evaluate the photoresponse by using a Xe lamp as the light source with radiation power of 100 mW/cm<sup>2</sup>.

After the fabrication of Cu<sub>2</sub>O/ $\gamma$ -FeOOH heterojunction, indium (In) electrodes with 1 mm<sup>2</sup> area each were evaporated on top of the heterostructure for electrical contacts in current density-voltage (J-V) characterization. Thus, the structure of the solar cell is In/Cu<sub>2</sub>O/ $\gamma$ -FeOOH/ITO. The photovoltaic properties of the Cu<sub>2</sub>O/ $\gamma$ -FeOOH solar cell were evaluated using a solar simulator under AM1.5 (100 mW/cm<sup>2</sup>) illumination condition. The

heterostructure were exposed to the irradiation from the ITO substrate side. Additionally, the interface of the heterojunction was studied by performing the X-ray photoelectron spectroscopic analysis using the XPS PHI-5000 (ULVAC-PHI) with Al K $\alpha$  as the X-ray source.

The galvanostatically electrodeposited Cu<sub>2</sub>O thin film displays polycrystalline cubic structure with preferred orientation along (111) similar to the reported XRD data for Cu<sub>2</sub>O in Ref. 14, while the as-prepared  $\gamma$ -FeOOH film shows nanocrystalline structure as reported in our previous work on this material (Ref. 20). The composition ratio (Fe/O) calculated from the AES data using the standard Fe<sub>2</sub>O<sub>3</sub> compound as a reference is about 0.51. Figure 1 shows the Fe 2p and O 1s XPS spectra for as-deposited  $\gamma$ -FeOOH film after 1.6 min of Ar ion bombardment. The sputtering is carried out to remove unwanted carbon impurities, which are detected at the surface located at binding energy (BE) of 285 eV. As displayed in Fig. 1, Fe 2p peaks are located at BE near 711.5 and 724 eV with satellite peaks near 715 and 730 eV, which signify the characteristics of Fe compounds. Furthermore, the O 1s spectrum seems to have two obvious peaks at BE closer to 530.2 and 531.9 eV. These peaks could be associated to oxide (O<sup>2-</sup>) and hydroxyl (OH) components of oxygen. Therefore, we could most likely consider that the as-deposited film is iron oxide hydroxide consistent with the composition obtained by AES and also with the Raman shifts reported in our previous studies on  $\gamma$ -FeOOH.<sup>20</sup>

Figure 2 shows the optical transmission and the band gap estimation for the as-prepared  $\gamma$ -FeOOH. The transmission is close to 65 % in the wavelength region from 800 – 1000 nm and the absorption edge is very apparent near 600 nm. By extrapolation of the linear region in the plot of  $(\alpha hv)^2$  versus  $hv$ , as depicted in the Tauc's plot in Fig. 2(b), the band gap is approximately 2.2 eV, which is similar to the reported band gap of the most popular iron compound,  $\alpha$ -Fe<sub>2</sub>O<sub>3</sub>.

Fig 3 depicts the PEC response of the  $\gamma$ -FeOOH film deposited at -0.9 (V vs SCE) under linearly increasing forward bias. As displayed in the figure, photocurrent density increases when illumination is turned on and decreases when in dark condition, i.e. generation of carriers by photo irradiation occurs. Since the photocurrent is positive, the photogenerated minority carriers are holes, i.e., the conductivity type is n-type.

Figure 4(a) shows the current-voltage characteristics for Cu<sub>2</sub>O/ $\gamma$ -FeOOH heterojunction measured under dark and light conditions. As shown in this figure, the rectification property and the increase in the current density under illumination are observed. In addition, the Cu<sub>2</sub>O/ $\gamma$ -FeOOH

heterostructure displays some photovoltaic characteristics as depicted in Figure 4(b). The solar cell parameters: open circuit voltage,  $V_{OC}$  and short circuit current density,  $J_{SC}$  are approximated to be 0.11 V and 0.95 mA/cm<sup>2</sup>, respectively. This result signifies that the  $\gamma$ -FeOOH could be applicable as n-type material in heterojunction solar cells.

Core-level spectroscopy is commonly used as a quantitative tool to study the interface between the individual components of the heterostructures.<sup>14, 21-23</sup> In view of the XPS signal intensity, the Fe 2p<sub>3/2</sub> and Cu 2p<sub>3/2</sub> levels are the better choice as core levels (CL). However, in the Cu<sub>2</sub>O/ $\gamma$ -FeOOH configuration, the overlapping of Fe 2p<sub>3/2</sub> peak with CuLM<sub>2,3</sub>M<sub>2,3</sub> Auger signals can be expected and this makes the use of (Fe and Cu) 2p levels difficult.<sup>24</sup> Hence, the (Fe and Cu) 3p levels are chosen as another option for CL. The valence and conduction band offsets of the Cu<sub>2</sub>O/ $\gamma$ -FeOOH heterostructure can be determined from the following relations:

$$DE_V = (E_{Cu\ 3p}^{Cu_2O} - E_V^{Cu_2O}) - (E_{Fe\ 3p}^{g-FeOOH} - E_V^{g-FeOOH}) - (E_{Cu\ 3p}^{hetero} - E_{Fe\ 3p}^{hetero}), \quad (1)$$

$$DE_C = (E_g^{Cu_2O} - E_g^{g-FeOOH}) + DE_V. \quad (2)$$

The expressions inside the parentheses in relation (1) are the energy difference between the core level and the valence band maximum (VBM) of individual materials and CL energy difference at the interface of the heterojunction.

Figures 5 and 6 depict the XPS spectra of the individual materials. The VBM spectrum for each layer with linear extrapolations of the leading edge for VBM determination (1.0 and 0.7 eV for  $\gamma$ -FeOOH and Cu<sub>2</sub>O, respectively) is also shown. The obtained VBM for Cu<sub>2</sub>O agrees well in the previous studies on Cu<sub>2</sub>O-based heterostructures (0.34 – 0.70 eV)<sup>14, 25</sup>. The energy difference between CL and VBM are estimated to be 55.2 eV for  $\gamma$ -FeOOH and 75.4 eV for Cu<sub>2</sub>O. Figure 7 shows the CL energy difference (equal to 19.4 eV) at the Cu<sub>2</sub>O/ $\gamma$ -FeOOH hetero-interface. According to relation (1),  $\Delta E_V$  is approximately 0.8 eV and considering the difference in the band gap between Cu<sub>2</sub>O (2.1 eV) and  $\gamma$ -FeOOH (2.2 eV as discussed above),  $\Delta E_C$  is approximately equal to 0.7 eV. Thus, a type II structure shown in Figure 8 is developed. As reported in Ref. 14,  $\Delta E_C$  is

about 0.5 eV for the Cu<sub>2</sub>O/ZnO hetero-interface, with the conduction band minimum (CBM) of Cu<sub>2</sub>O higher than that of ZnO. Thus CBM position of  $\gamma$ -FeOOH is rather close to that of ZnO.

In summary,  $\gamma$ -FeOOH thin films displayed suitable characteristics for solar cell applications. As-deposited  $\gamma$ -FeOOH exhibited n-type conductivity and the optical band gap was around 2.2 eV. Successful fabrication of Cu<sub>2</sub>O/ $\gamma$ -FeOOH heterojunction was demonstrated by employing facile galvanostatic-potentiostatic electrodeposition techniques. The formed p-n junction between Cu<sub>2</sub>O and  $\gamma$ -FeOOH is considered to be the first p-n junction based on any Fe compounds. Photovoltaic characteristics were confirmed for Cu<sub>2</sub>O/ $\gamma$ -FeOOH heterojunction with  $V_{OC} = 0.11$  V and  $J_{SC} = 0.95$  mA/cm<sup>2</sup>. Photoelectron spectroscopy predicted that the CBM of Cu<sub>2</sub>O is higher than that of  $\gamma$ -FeOOH by 0.7 eV. Hence, a type II heterostructure was developed. The above findings open alternative options in choosing oxide semiconductor as n-type or as buffer layer in the fabrication of heterojunction solar cells.

The authors would like to thank Mr. Y. Moriguchi for his technical assistance in XPS measurement and Dr. M. Kato for his useful suggestions.

- 1) V. Georgieva and M. Ristov: *Sol. Energy Mater. Sol. Cells* **73** (2002) 67.
- 2) P. E. de Jongh, D. Vanmaekelbergh, and J. J. Kelly: *Chem. Mater.* **11** (1999) 3512.
- 3) T. Mahalingam, J. S. P. Chitra, S. Rajendran, and P. J. Sebastian: *Semicond. Sci. Technol.* **17** (2002) 565.
- 4) P. E. de Jongh, D. Vanmaekelbergh, and J. J. Kelly: *J. Electrochem. Soc.* **157** (2) (2000) 486.
- 5) Y. Song and M. Ichimura: *Int. J. Photoenergy* **2013** (2013) 1.
- 6) S. Noda, H. Shima, and H. Akinaga: *J. Phys.: Conf. Series* **433** (2013) 012027.
- 7) S. K. Baek, K. R. Lee, and H. K. Cho: *J. Nanomater.* **2013** (2013) 1.
- 8) J. Cui and U. J. Gibson: *J. Phys. Chem. C* **114** (2010) 6408.
- 9) K. Fujimoto, T. Oku, and T. Akiyama: *Appl. Phys. Express* **6** (2013) 086503.
- 10) M. Izaki, T. Shinagawa, K. Mizuno, Y. Ida, M. Inaba, and A. Tasaka: *J. Phys. D* **40** (2007) 3326.
- 11) J. Katayama, K. Ito, M. Matsuoka, and J. Tamaki: *J. Appl. Electrochem.* **34** (2004) 687.
- 12) J. Cui and U. J. Gibson: *J. Phys. Chem. C* **114** (2010) 6408.
- 13) T. Minami, Y. Nishi, T. Miyata, and J. Nomoto: *Appl. Phys. Express* **4** (2011) 062301.
- 14) M. Ichimura and Y. Song: *Jpn. J. Appl. Phys.* **50** (2011) 051002.
- 15) T. Minami, Y. Nishi, and T. Miyata: *Appl. Phys. Express* **6** (2013) 044101.
- 16) L. Panadimitriou, N. A. Economou, and D. Trivich: *Solar Cells* **3**, (1981) 73.
- 17) H. Naono and K. Nakai: *J. Colloid Interface Sci.* **128** (1989) 146.
- 18) S. B. Rawal, A. K. Chakraborty, and W. I. Lee: *Bull. Korean Chem. Soc.* **30** (11) (2009) 2613.
- 19) Y. Jia, T. Luo, X.-Y. Yu, Z. Jin, B. Sun, J.-H. Liu, and X.-J. Huang: *New J. Chem.* **37** (2013) 2551.
- 20) J. J. M. Vequizo and M. Ichimura: *Appl. Phys. Express* **6** (2013) 125501.
- 21) E. A. Kraut, R. W. Grant, J. R. Waldrop, and S. P. Kowalczyk: *Phys. Rev. B* **28** (1983) 1965.
- 22) B. Kramm, A. Laufer, D. Reppin, A. Kronenberger, P. Hering, A. Polity, and B. K. Meyer: *Appl. Phys. Lett.* **100** (2012) 094102.
- 23) A. J. Nelson : *J. Appl. Phys.* **78** (1995) 5701.
- 24) G. Polzonetti, V. Di Castro, and C. Furlani: *Surf. Inter. Anal.* **22** (1994) 211.
- 25) M. Yang, L. Zhu, Y. Li, L. Cao, and Y. Guo: *J. Alloys and Compounds* **578** (2013) 143.

Fig. 1 (a) Fe 2p and (b) O 1s spectra for the as-deposited  $\gamma$ -FeOOH thin film after sputtering.

Fig. 2 (a) Optical transmission and the (b) corresponding Tauc's plot for the as-deposited  $\gamma$ -FeOOH thin film.

Fig. 3 PEC response for the as-deposited  $\gamma$ -FeOOH thin film under linearly increasing bias.

Fig. 4 (a) J-V characteristics for  $\text{Cu}_2\text{O}/\gamma$ -FeOOH heterojunction with 50 nm-thick  $\gamma$ -FeOOH under dark and light conditions and (b) the region near 0 V of the J-V curve under illumination.

Fig. 5 (a) Fe 3p and (b) VBM spectra for the as-deposited for the  $\gamma$ -FeOOH thin film deposited at -0.9 (V vs SCE).

Fig. 6 (a) Cu 3p and (b) VBM spectra for the as-prepared  $\text{Cu}_2\text{O}$  thin film deposited on ITO substrate at  $-1.0 \text{ mA/cm}^2$ .

Fig. 7 (Cu-Fe) 3p spectrum at the interface of the electrodeposited  $\text{Cu}_2\text{O}/\gamma$ -FeOOH heterojunction.

Fig. 8 Band alignment diagram for the electrodeposited  $\text{Cu}_2\text{O}/\gamma$ -FeOOH heterojunction.  $E_C$  and  $E_V$  are conduction band minimum and valence band maximum, respectively.



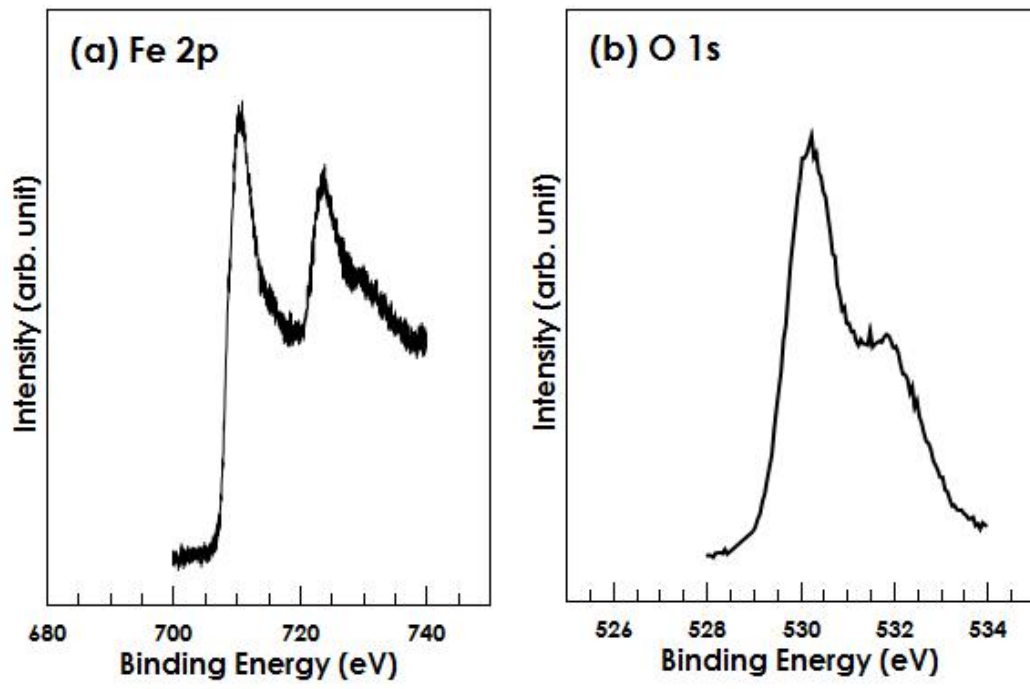


Fig. 1

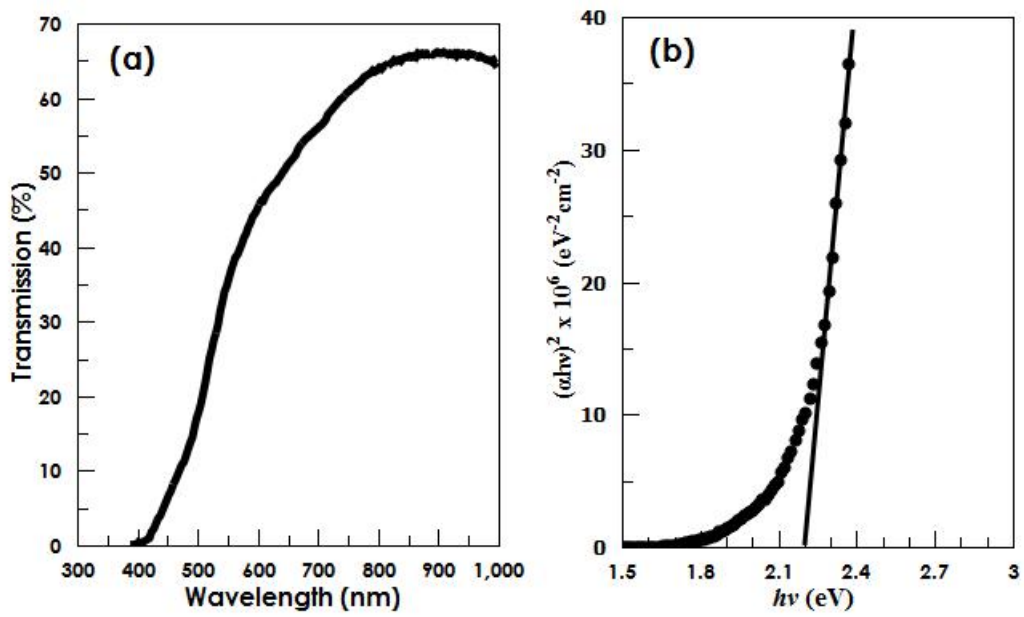


Fig. 2

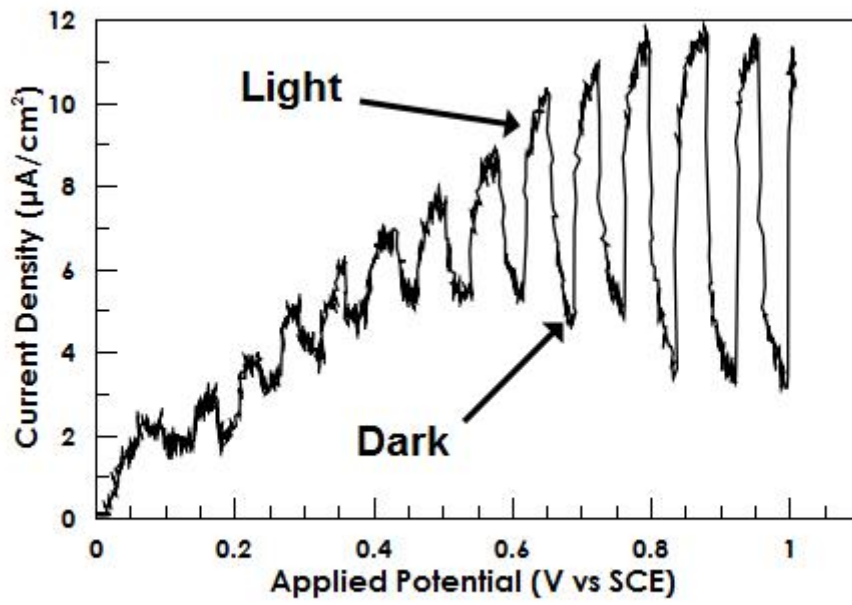


Fig. 3

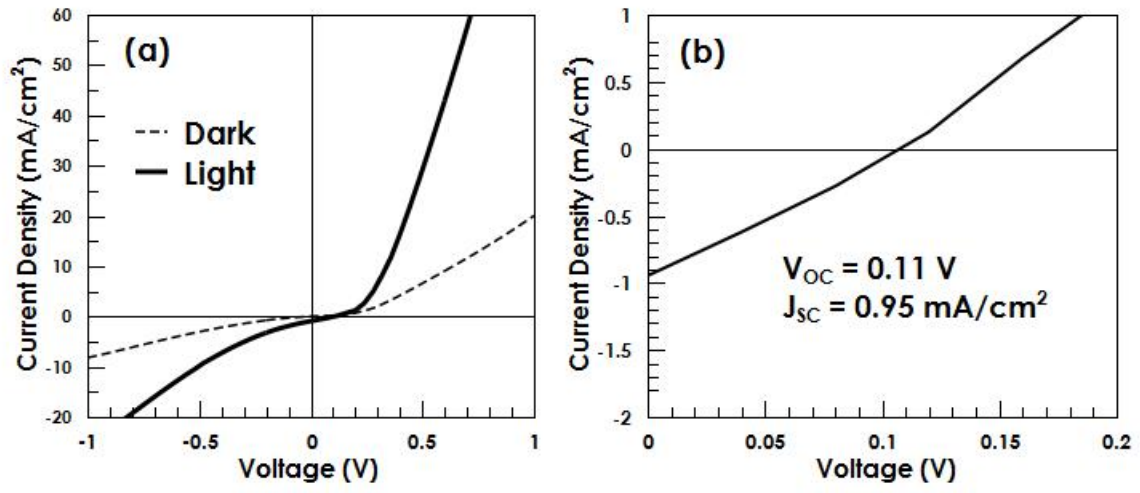


Fig. 4

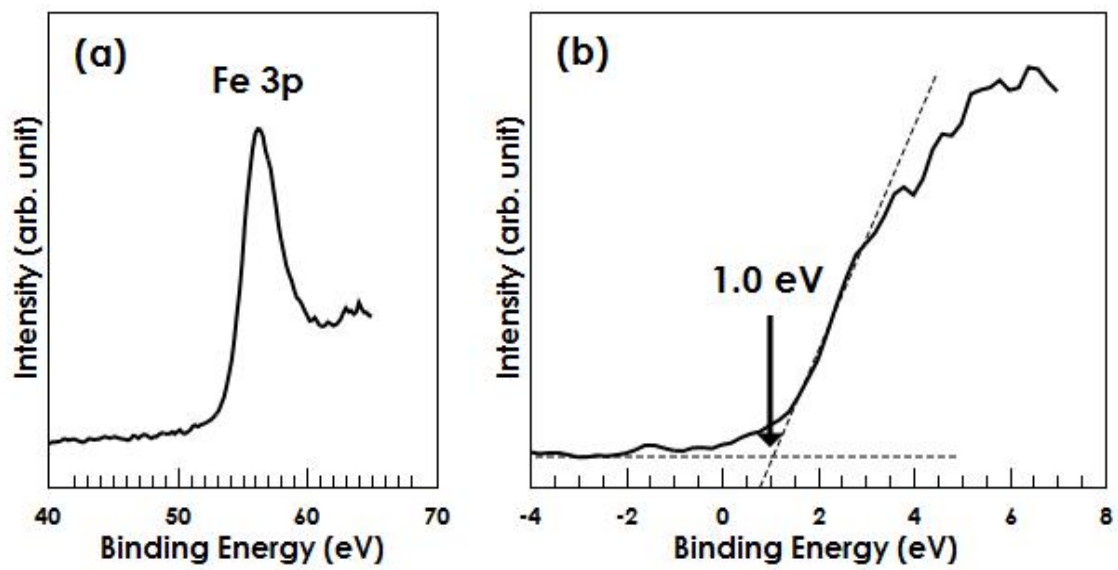


Fig. 5

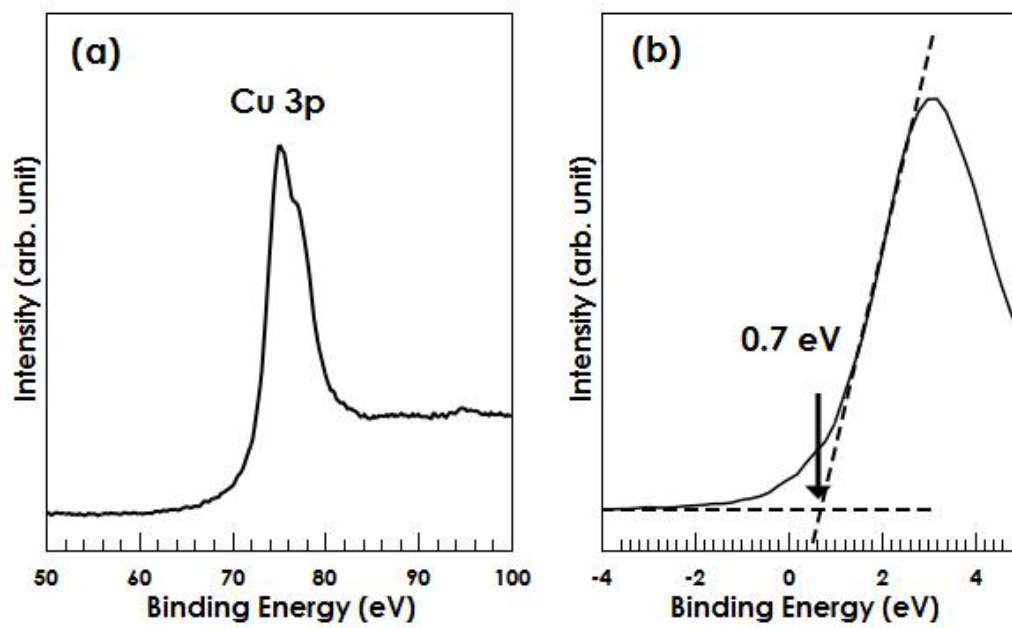


Fig. 6

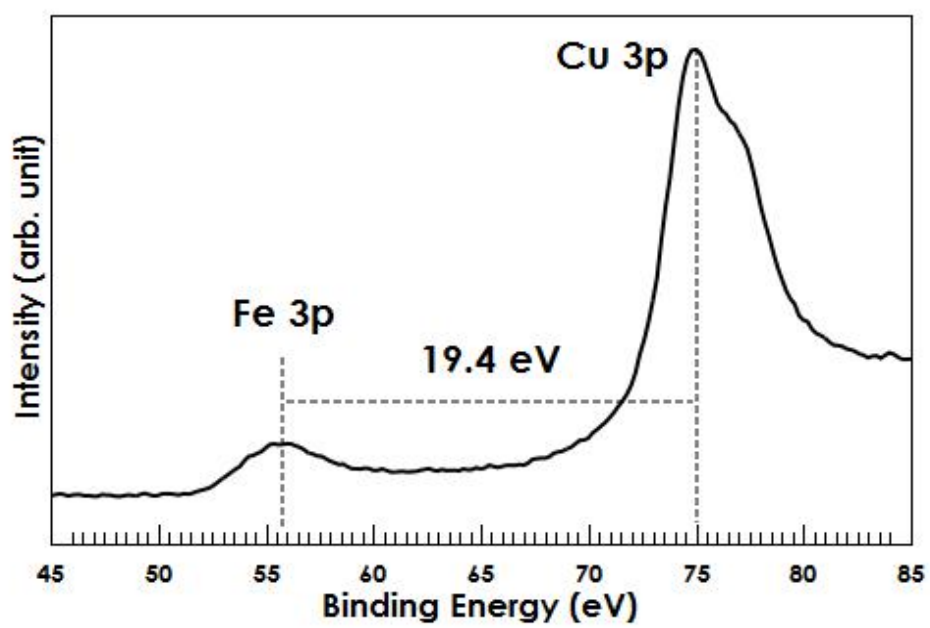


Fig. 7

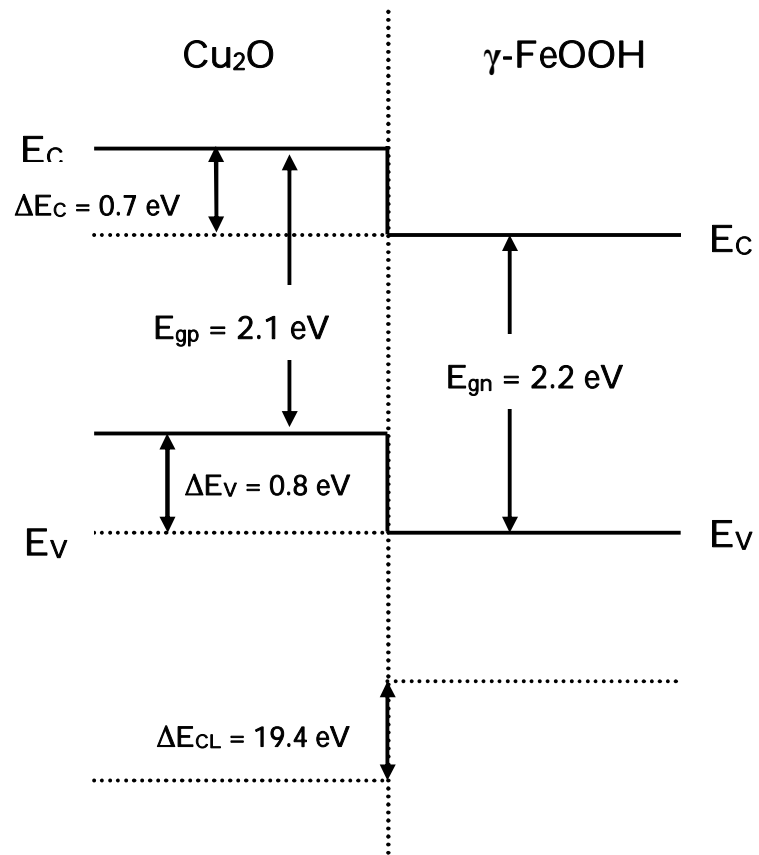


Fig. 8